RSC Advances

ROYAL SOCIETY OF CHEMISTRY

www.rsc.org/advances

Characterization of electrical surface properties of mono- and co-cultures of *Pseudomonas aeruginosa* and methicillin-resistant *Staphylococcus aureus* using Kelvin probe force microscopy

Author information

Eric Birkenhauer, BioNano Laboratory, School of Engineering, University of Guelph, Guelph, Ontario, Canada.

Suresh Neethirajan (Assistant Professor, Ph.D., P. Eng.: sneethir@uoguelph.ca), BioNano Laboratory, School of Engineering, University of Guelph, Guelph, Ontario, Canada.

Abstract

Microbial attachment is the first and only reversible step in biofilm formation and the physical attributes of the substrate surface play a crucial role in the attachment process. Medically relevant surfaces such as clean stainless steel and gold surfaces exhibit negative surface potentials and inhibit microbial attachment. Poly-L-lysine functionalized surfaces have positive surface potentials and promote the rapid attachment of microbes after 30 minutes. KPFM analyses revealed that the cell surface potentials for all species (*Pseudomonas aeruginosa* and MRSA) and culture conditions were affected by the type of substrate used. Co-culturing in-vitro, which mimics the in-vivo situation, is a critical factor determining the observed shifts in surface potential for MRSA, significantly affecting its cellular activity. Selective plating experiments further confirmed the growth inhibition of MRSA in the presence of *P. aeruginosa*. Under KPFM measurement conditions it was revealed that both microbial species show positive cell surface potentials, with the exception of MRSA on gold surface. No morphological changes were observed in both mono or co-cultured *P. aeruginosa* and MRSA as observed by atomic force microscopy. Zeta potential measurements on cultures revealed negative zeta values. This study provides an insight into the electrokinetic dynamics of surfaces and its consequence on the attachment of virulent bacteria. The study further highlights the importance of physical attributes such as surface charge, that could be exploited for the development of therapies involving nanocoatings or electrical fields in order to prevent microbial attachment and the formation of recalcitrant wound biofilms.

Introduction

The study of chronic wounds, non-healing bacterial infections, and the body's response in relation to invading and colonizing microorganisms is of great concern to healthcare systems.

Chronic infections, unlike acute infections, can last for months to years in individuals with compromised health (i.e. diabetics, cancer patients, etc.), severe traumatic injuries (i.e. military combat related injuries), or burns.[1-3] Chronic illness leads to increased morbidity in patients, further placing strain on healthcare systems. Biofilms present in wound sites represent extensive microbial contamination and colonization. If left untreated in compromised individuals, it can result in sepsis and the possible loss of human life.[2] Microorganisms that naturally inhabit our bodies belong to our host microbiome. Under normal circumstances these microbes are restricted, almost exclusively, to mucosal sites. These include surfaces of the body exposed to the outside world (i.e., skin, gastrointestinal tract, oral cavity, upper respiratory tract, and distal regions of the reproductive system).[2, 4] These surfaces exert selective pressures on the microbes in order to prevent infection and colonization. As is observed in the case of epithelium, this may include the production of sweat, sloughing of keratinocytes in the stratum corneum, and antigen-presenting cells (i.e., Langerhans cells).[1, 2] Wounds, or breaks in the epidermis (epithelial or dermal regions) result in molecular cascades that almost immediately act to repair wounds and prevent microbial colonization. This may include altered antimicrobial peptide expression, an influx of macrophages to the site of damage (increased levels of extracellular signal molecules associated with damage such as cytokines, chemokines, eicosanoids, etc., help to attract macrophages), clotting or coagulation, leukocyte recruitment, fibroblast proliferation and collagen production (scarring), and regeneration of damaged basal layers/membranes (depending on extent and depth of wounding).[13]

Microorganisms also rarely exist in their planktonic state or as single-species in natural environments. The majority of microbial communities may consist of multiple species of bacteria, fungi, and viruses, creating polymicrobial environments. A large scale analysis of

diabetic wound biofilms showed that 16.2% of biofilms contained one bacterial isolate, 20.4% contained two bacterial isolates, 19.7% had three, 13.3% had four isolates, and 30.4% were found to contain five or more bacterial isolates.[2] Of the microorganisms isolated, most were found to be host-associated opportunistic pathogens. In cases where a bacterial cell becomes attached to abiotic or biotic (i.e. wound) surfaces, they may excrete a hydrated matrix, often consisting of various polysaccharide and protein compounds[1]. This matrix is collectively known as an extracellular polymer substance (EPS). Formed EPS matrices act to entrap other microorganisms.[1] In individual bacterial biofilms there may exist a variety of interactions between different species and organisms. These could include bacterial-bacterial, bacterial-fungal, and bacterial-viral interactions.[1] Each type of microbial interaction and the microbial load of different species make every newly formed biofilm unique from those previously encountered. Due to the multitude of interactions within the biofilms at the cellular level, quorum sensing is crucial in order to maintain biofilm integrity and minimize competition between microorganisms. Besides harboring external microorganisms, biofilms also act to promote cell differentiation.[2] Biofilms can also serve as shields to protect its constituents from undesired environmental changes, such as rapidly shifting environmental pH, nutrient deprivation, disinfectants, antimicrobials (chemical or peptide), and physical forces.[2]

Many of the physical and chemical characteristics of an attachment surface act as important criterion in determining the initial growth of a biofilm. Biofilm development occurs in 5 stages: (1) attachment/adhesion, (2) colonization/EPS production, (3) continued growth, (4) macro colony formation and maturation, and (5) the development of tertiary structures, phenotypically differentiated cells, and dispersal.[5] If the environment and surface conditions are optimal, the microorganisms attach to the substrate surface irreversibly, followed by replication and excretion

of EPS. Attachment/adhesion (1) is the only reversible step in the biofilm formation process and is therefore the most important in regards to this study.[5]

Pseudomonas aeruginosa and methicillin-resistant *Staphylococcus aureus* (MRSA) are two of the most common microorganisms responsible for nosocomial and non-healing bacterial biofilms.[3, 6] Both *P. aeruginosa* and MRSA are opportunistic pathogens and are prevalent due to their capacity to rapidly form biofilms (*P. aeruginosa* has been shown to form biofilms in less than 10 hours *in vitro* on plastic cover slips).[4, 7] *P. aeruginosa* and MRSA utilize different methods for adhesion to the surface substrates. *P. aeruginosa* utilizes type-IV pili while MRSA relies heavily on adhesion proteins (i.e. adhesins, Clumping factor B (ClfB), Extracellular adherence protein (Eap)), and surface properties (charge, hydrophobicity, roughness, etc)[8-10]. *P. aeruginosa* is known to express virulence factors such as exotoxin A, exoenzyme S, and pyocyanins which increase its pathogenicity by inducing apoptosis in macrophages and neutrophils, while pyocyanin compounds inhibit the growth of competing microorganisms.[3, 11]

MRSA infections are well-documented in chronic as well as acute wounds.[12] MRSA is known to produce a plethora of toxins including Panton-Valentine leukocidin (PVL), staphylococcal protein A (SpA), and α-hemolysin (hla), which are collectively responsible for its increased virulence and pathogenicity.[3] These compounds are up-regulated in polymicrobial environments.[3] Studies examining the interaction of *P. aeruginosa* and MRSA have revealed that both species, individually and together, delay wound closure.[2, 3] *P. aeruginosa* and MRSA have been shown to act competitively in co-culture, with *P. aeruginosa* playing a dominant role.[3, 4] *P. aeruginosa* has been shown to significantly inhibit the growth of MRSA growth. It however does not stop the growth of MRSA. Biofilm forming strains of *P. aeruginosa* significantly outcompete MRSA in co-culture and have been shown to alter MRSA colony

morphology, producing MRSA small colony variants.[4] Biofilms containing both *P. aerugionosa* and MRSA can also be differentiated from their single-species counterparts.[4] *P. aeruginosa* has also been shown to protect MRSA, specifically against *Dicytostelium discoideum* phagocytosis in co-culture.[4] *P. aeruginosa* and MRSA together also suppress keratinocyte growth factor 1 in *in-vivo* wound models, which further delays the process of wound healing and epithelial regeneration.[3] Adhesion of MRSA and PA onto wound tissue matrices depends on multiple factors and surface charge is one important influencing factor.

There are several studies examining the molecular, genetic, and physiological interactions between *P. aeruginosa* and MRSA in co-culture. However, in this study we examine the effects of mono/co-culturing and surface substrate electrical charge on microbial culture and cell surface charges. This was accomplished using a combination of atomic force microscopy (AFM), Kelvin probe force microscopy (KPFM, a module of AFM), and dynamic light scattering (DLS). AFM is a non-optical microscopy tool, belonging to the family of scanning probe microscopes, with many applications in the examination of biological systems.[13] AFM is most popularly used for cell topography imaging; however many modules allow for analysis of physicomechanical and physicochemical processes and include force spectroscopy, molecule interaction analysis (protein-ligand analysis of binding affinity), live-action analysis (high-speed AFM can be used to capture videos of biological processes such as the movement of myosin V along actin filaments), to name a few.[13-17] There are many dynamic modules of AFM which allow for near limitless experimentation.

In the KPFM module of AFM, the contact potential difference (CPD) between two surfaces is measured.[18, 19] KPFM relies on a conductive cantilever (commonly Pt coated) and ideally a conductive surface.[18] A known AC bias is applied to the cantilever tip in order to generate a

current flow between the tip and sample.[18, 19] The tip is brought close enough to the sample such that the sample and tip represent a parallel plate capacitor. Changes in the CPD between the AFM cantilever tip and sample result in the flex, and these flexural changes in the cantilever are nullified by applying a DC voltage bias that is equal and opposite in magnitude to the experienced CPD.[18] Information about the DC voltage required to nullify the resultant CPD flexural force is subsequently converted into an electrical surface potential map image. In one-pass KPFM scan modes, which include amplitude and frequency modulation modes (AM-KPFM and FM-KPFM, respectively) the cantilever is oscillated at two frequencies in order to simultaneously obtain the topography and surface potential data.[18, 19] Lift mode is a two-pass scan mode version of KPFM, in which after a single scan of the topography the tip is raised 10 – 100 nm above the surface and scanned back across the same area.[19] Lift mode does not require the application of an AC voltage to the cantilever tip in order to generate current flow, and is used more-so for the examination of electrostatic forces. Work has been done for application of KPFM in non-polar solutions, however KPFM has not been used for imaging in highly ionic polar solutions (ideal for cell growth and maintenance) due to the application of bias feedback voltages on the cantilever, therefore KPFM imaging of live cells has not currently been accomplished[20-23]. KPFM imaging can also be accomplished on non-conductive samples as long as there is an underlying conductive material and the non-conductive sample is thin.[24-26] For this study, we utilized FM-KPFM as it has been shown to provide superior resolution for biological samples.[19]

AFM and KPFM have been used to study the effects of surface substrate characteristics on the attachment and growth of biological specimens.[24, 27, 28] Previous research has shown that electrically homogeneous surfaces with increased porosity and hardness, decreased

hydrophobicity, and positive surface potential improve microbial attachment to surfaces.[24, 26, 27, 29-31] It has also been shown that aside from chemical and cytokine interactions at the wound site, endogenous electrical fields are generated by the epithelium in response to injury.[32] These endogenous electrical fields help to recruit and coordinate immune and epithelial cells to sites of injury.[32] Electrical stimulation is now being considered as a potential therapeutic treatment for wound healing and as a preventative measure for microbial attachment/biofilm formation.[32]

For FM-KPFM in this research, *P. aeruginosa* and MRSA were plated on poly-L-lysine coated stainless steel and gold surfaces. Stainless steel was utilized due to its medical relevance (hypodermic needles, catheters, sensors, probes, orthopedic implants, scalpels, etc.) while gold was utilized as a comparative surface substrate. The aim of this research is to understand the effects of substrate surface potential on microbial attachment and the effects *P. aeruginosa* and MRSA growth in mono- and co-culture on cell surface potential. AFM analysis of representative cells from mono- and co-cultures was also done to determine the effects of co-culturing on cell morphology. DLS was used as a comparative method for measuring the electrical properties (zeta potential) of cell cultures. Selective plating experiments were also carried out, with competitive index (CI) and relative increase ratio (RIR) of MRSA being calculated in order to further understand the competitive effects between MRSA and *P. aeruginosa*.

Results and discussion

There are numerous studies examining the genetic and physiological interactions of MRSA and *P. aeruginosa* as well as their implications on the wound healing process.[1, 3, 4]

However, the physical factors influencing the attachment of virulent bacteria such as *P. aeruginosa* and MRSA, as well as the effects of existence of both *P. aeruginosa* and MRSA on

the attachment properties and the surface charge of the substrate surface have not been adequately addressed. Previous work has demonstrated that bacterial surface charge is not only related to its envelope structure, but also to its interactions with natural surfaces in the environment.[33] Here we apply FM-KPFM as a technology to advance our understanding of inter-microbial and microbial-surface interactions at the micro (cell-cell) and nanoscale levels. FM-KPFM provides the ability to measure the surface potential of individual cells, through the generation of surface potential maps as can be seen in **Fig. 1**. FM-KPFM in most cases requires the cantilever tip and sample surfaces to be conductive. Stainless steel and gold are excellent materials in this regard to study adhered mono- and co-cultures of *P. aeruginosa* and MRSA. Co-culturing (1:1 ratio of inoculums) experiments were carried out due to their relevance in nosocomial environments, with a focus on cutaneous wounds, in which prolonged microbial infections are rarely found as mono-cultures. Therefore, a co-culture mimics a more realistic situation in which *P. aeruginosa* and MRSA are likely to interact. Co-culturing experiments also help us determine if there were any changes between cell surface potentials, culture zeta potentials, and cell morphologies in comparison to individual mono-cultures. Furthermore, co-culturing experiments were also used to evaluate the extent to which co-culturing affected *P. aeruginosa* and MRSA cell growth. Selective plating experiments revealed the nature of the competitive relationship between *P. aeruginosa* and MRSA by evaluating the CI and RIR from CFU/mL data.

AFM and FM-KPFM work revealed the effects of surface substrate charge on microbial attachment, as well as the surface charges on the microbial cell surface during mono- and co-culturing, and allowed for cell dimensional analysis. FM-KPFM data collected from cells on both stainless steel and gold substrates is depicted in **Fig. 2**. Initial attempts to adhere *P.*

aeruginosa and MRSA cultures on clean stainless steel and gold surfaces were unsuccessful even after 3 hours of static incubation. After this time period no microbial cells were visible from AFM scans. FM-KPFM measurements of the clean surface substrate revealed overall negative surface potentials on 5 µm x 5 µm areas, with a significant difference observed between stainless steel and gold surfaces (-0.045 V and -0.126 V, respectively, P = 0.047). It is known that microorganisms in liquid cultures generally have negative surface potentials (due to the presence of negatively charged phosphate groups and teichoic acid in Gram negative and Gram positive microorganisms, respectively in the outer membrane/wall composition), with some exceptions.[34-36] Thus, it was understandable that no microbial attachment was seen on negatively charged surfaces. We then functionalized the surfaces with poly-L-lysine, a known adhesion polymer used in cell culturing, and FM-KPFM scans of 5 µm x 5 µm areas showed a surface potential shift to positive values for both stainless steel and gold attachment surfaces (0.133 V and 0.126 V, respectively). We optimized the protocol such that the microbial cultures were plated for 30 minutes before FM-KPFM analysis. This time period was chosen as longer times (40 minutes +) resulted in cell overcrowding. Even with a short incubation time on substrate surfaces, significant differences in membrane surface potentials were observed between cells in mono- and co-cultures.

As seen in **Fig. 2**, a comparison of *P. aeruginosa* in mono- and co-culture revealed significant differences between cell surface potentials on stainless steel and gold substrates. For *P. aeruginosa* mono-cultures, positive cell surface potentials were observed on both stainless steel and gold substrates (0.218 V and 0.154 V, respectively, P = 0.016). A similar trend was observed for *P. aeruginosa* cells in co-culture on stainless steel and gold substrates (0.286 V and 0.150 V, respectively, P < 0.001). In both cases, higher cell surface potentials were observed for

P. aeruginosa on stainless steel substrates, implying that the type of substrate influences cell surface potential in both mono-and co-cultures. Comparing *P. aeruginosa* cells on similar substrates from mono- and co-cultures helped determine the effects of co-culturing on surface potential. A significant increase in cell surface potential was observed between mono- and co-cultured *P. aeruginosa* on stainless steel substrates ($P = 0.003$), while no significant difference was observed on gold substrates.

MRSA in mono and co-culture, showed significant differences between cell surface potentials on stainless steel and gold substrates, and between cells in mono- and co-cultures. The most dramatic example of substrate-type effect on cell surface potential was observed in MRSA mono-cultures. Mono-cultures on stainless steel and gold showed surface potentials of 0.160 V and -0.025 V, respectively ($P < 0.001$). This dramatic shift from positive cell surface potential on stainless steel to negative cell surface potential on gold helps further confirm the ability of substrate-type to affect various cell aspects, including development, growth, adherence, morphology, and most importantly metabolism, which has been correlated to changes in cell membrane surface potential through the redistribution of proteins in cell membranes.[26] Overall, MRSA on stainless steel exhibited higher cell surface potentials. Large positive charges were seen for MRSA in co-culture on both substrate types (stainless steel = 0.327 V, gold = 0.259 V). Cell surface potentials for MRSA in co-culture were also found to be significantly different between the two substrate types ($P < 0.001$).

On comparison between mono- and co-cultures on similar substrates, significant increases in surface potentials were observed for MRSA, both on stainless steel and gold substrates ($P < 0.001$ in both cases).

From these FM-KPFM results (**Fig. 2**), it is apparent that the substrate type exhibits a significant influence on the cell surface potential. However, co-culturing has a greater effect on MRSA cell surface potential. Although co-culturing did not exhibit a significant effect on the surface potential of *P. aeruginosa*, it is noteworthy that *P. aeruginosa* being the dominating species in the co-culture should be less affected by MRSA. MRSA is the susceptible species in this co-culture for reasons described previously.[3, 11] These competitive effects can be seen in **Fig. 3**. The CI and RIR calculations, from selective plating experiments, provide insight into the exact nature of the ability of a species to compete.[37] CI and RIR calculations were determined with regard to the CFU/mL of the susceptible species, which in this case was MRSA. MRSA exhibited a RIR value above 1 (1.646), indicating that MRSA grew faster than *P. aeruginosa* in mono-culture. As expected, MRSA exhibited a CI below 1 (0.382), indicating that MRSA in co-culture competed poorly in comparison to *P. aeruginosa* (**Fig. 3**). Our findings confirm previous studies that have shown *P. aeruginosa* to outcompete MRSA in co-culture.

AFM images were obtained from mono- and co-cultured *P. aeruginosa* and MRSA cells adhered to gelatin-coated mica to see if co-culturing led to any significant changes in the cell morphology of *P. aerugionosa* and MRSA. **Table 1** shows the average dimensions (length, width, and diameter) of both cell types from mono- and co-cultures. It was observed that co-culturing did not lead to any significant changes in cell dimensions, implying that co-culturing does not result in noticeable physical changes in *P. aeruginosa* and MRSA cells. Thus, we conclude that inhibitory effects of *P. aeruginosa* on MRSA are not associated with, or cause morphological changes in MRSA cells.

As an alternative method for indirectly determining cell surface charge, DLS was employed to determine cell culture zeta potentials in PBS (**Fig. 4**). Other methods such as culture isoelectric

point determination offer more crude measurements of whole culture electrical potentials. However, unlike isoelectric point determination, zeta potential is more accurate as it is accomplished by measuring the distances between particles ranging from 3.8 nm – 100 µm (specific to the Malvern Instruments Zetasizer Nano Z) in a solution surrounding colloidal particles (i.e. bacterial cells).[38, 39] This is different from a direct measurement of cell surface potentials. Around every bacterial cell in solution there exists a liquid layer of charged particles.[38-40] One of these layers, the stern layer immediately surrounding the cells surface contains strongly bound ions. Since most microorganisms are negatively charged, particles in the stern layer are generally positively charged. Outside the stern layer exists an electrical double-layer, where both negative and positive ions are found [38]. Particles in this layer are not bound tightly to the stern layer. When the cell moves in solution, this layer moves with it. The electrical potential on the boundary of this layer and the immediate liquid surrounding it is where the zeta potential is determined from the electrophoretic mobility of cells in an electric field. Factors such as cell surface charges and other cell properties (i.e., elasticity of the cell, species heterogeneity) influence the width of the electrical double layer.[38, 39] This is one reason why heterogeneous microbial species (i.e. those expressing various pili/fimbriae types) can, in some cases, exhibit two zeta potential peaks.[38, 40] To our knowledge, this has not been observed with *P. aeruginosa* or MRSA cells previously and was not observed in our experiments [41-43]. Zeta potential experiments showed negative potentials for all culture types (*P. aeruginosa*, MRSA, and co-culture) ranging from -12.233 mV to -13.483 mV, with no significant differences between cultures **(Fig. 4)**. Negative zeta potentials of the studied species were expected.[41-43] It should be noted that zeta potential measurements and FM-KPFM data are not comparable and zeta potential measurements represent a more accurate estimate of cell surface potential as *P.*

aeruginosa and MRSA are in their native state. Sample preparation for FM-KPFM requires that cells be dried on surface substrates. Therefore, information collected on these dead cells using FM-KPFM can only be used for describing general trends on the effects of surface type and co-culturing on shifts in cell surface potential. The cell surface potentials observed in FM-KPFM do not accurately represent the cell surface potential of *P. aeruginosa* and MRSA in a wound setting or on medical equipment that may contain stainless steel or gold surfaces. As previously mentioned, efforts are being made to develop KPFM technology for imaging of live cells in liquids. However, this technology does not currently exist.

Experimental

Bacterial strains, culture conditions, and mono- and co-culture preparation

Pseudomonas aeruginosa BK-76 and MRSA USA100 strains were used throughout the entirety of this work. *P. aeruginosa* BK-76 was isolated from a canine ear skin infection. MRSA USA100 is a commonly known MRSA strain that was originally isolated from a human skin infection. MRSA and *P. aeruginosa* strains were streaked from frozen cultures stored at -80ºC, onto 5% sheep blood agar plates (SBA). Plates were incubated at 37ºC in inverted positions for 24 hours. Liquid cultures were generated in tryptic soy broth (TSB, 6 mL) by inoculating with single colonies from SBA plates. TSB cultures were then grown in a reciprocal shaker at 200 rpm at 37ºC for 24 hours.

Co-cultures were generated from 24 hour liquid cultures. 24 hour cultures were standardized to a 0.5 McFarland standard (~1.5 x 10^8 CFU/mL) in TSB. From standardized cultures, 1 mL was taken from *P. aeruginosa* BK-76 and MRSA USA100 and inoculated into 6 mL of fresh TSB (8

mL total after both inoculations). Co-cultures were then incubated in a reciprocal shaker at 200 rpm at 37ºC for 24 hours.

For selective plating studies, 1 mL of standardized (0.5 McFarland) mono- and co-cultures were re-inoculated into 6 mL fresh TSB and incubated under previously described conditions for another 24 hours so as to know the initial inoculum concentrations at time 0 hour. 10^{-1} – 10^{-8} dilutions of microbial cultures, diluted in phosphate buffered saline (PBS, pH = 7.4), were used for selective plating experiments (performed in triplicate). Mono-cultures were plated on SBA plates while co-cultures were plated on Pseudomonas CFC Agar (Oxoid) and Staphylococcus Medium 110 (Oxoid) in order to select for *P. aeruginosa* and MRSA cells. Plates with 25 – 250 colonies were used for determining CFU/mL values. CFU/mL values at 0 hour and 24 hour time points were then used to determine CI and RIR for MRSA.

For zeta potential measurement experiments (done in triplicate), 24 hour mono- and co-cultures were washed twice (centrifuged at 5000 rpm for 3 minutes) in deionized H_2O and re-suspended in PBS. Re-suspended cells were then standardized to a 0.5 McFarland standard in fresh PBS. The zeta potential of these samples was measured using DLS.

Stainless steel and gold substrate preparation for AFM/KPFM

Stainless steel and gold AFM sample disks (20 mm and 10 mm diameters, respectively) were purchased from TED PELLA Inc. Prior to poly-L-lysine functionalization and microbial inoculation, sample disks were washed with 5 mL deionized H_2O on front- and backsides, followed by sonication for 1 min. After washing and sonication, sample disks were allowed to dry overnight. To dry sample disks, 200-400 µL of 0.1% poly-L-lysine (w/v in H_2O) was applied and allowed to sit at room temperature, on the sample disks, for 1 hour. Disks were

subsequently washed with 1 mL of deionized H_2O and allowed to dry at room temperature. Once dry, 200-400 µL of 2x washed (in deionized H_2O, centrifuged at 3000 rpm for 3 minutes) was plated onto sample disks for 30 minutes and afterwards washed with 1 mL deionized H_2O. Inoculated sample disks were allowed to dry overnight at room temperature before imaging.

AFM/FM-KPFM imaging

All AFM/FM-KPFM imaging was performed using an Agilent 5500 series ILM-AFM under ambient conditions. Platinum-coated conductive DPE (low noise) cantilevers (Mikromasch) were used, with an average resonant frequency, spring constant, and tip-apex diameter of 80 kHz, 2.7 N/m, and 40 nm, respectively. To obtain high resolution, low noise, AFM/FM-KPFM images 512x512 resolution images ranging from 5 µm x 5 µm to 10 µm x 10 µm were collected at raster scan speeds of 0.02-0.05 lines/seconds, with a set cantilever frequency of 5 kHz being used for FM-KPFM data collection. Integral and proportional gains for FM-KPFM were set at a 0.3% for all images with a bandwidth of 2 kHz. FM-KPFM image analysis was done using Agilent Pico Image software. Data taken from 15 cells were used for analysis of overall cell surface potential. Determination of average cell dimensions from AFM images between individual cell types in mono- and co-cultures was done using 5 representative cells from each species.

Competitive index and relative increase ratio calculations

To determine the effects of *P. aeruginosa* on MRSA microbial growth in mono-culture vs. co-culture, competitive index and relative increase ratios were determined by comparing initial inoculum CFU/mL rates to CFU/mL rates of both species after 24 hours. CI values of MRSA on *P. aeruginosa* were calculated, using co-culture data, by dividing the ratio of MRSA CFU/mL:

P. aeruginosa CFU/mL at 24 hours by the ratio of MRSA CFU/mL: *P. aeruginosa* CFU/mL at 0 hours. RIR of MRSA was determined by dividing MRSA CFU/mL rates from mono-cultures after 24 hours by CFU/mL rates of *P. aeruginosa* in mono-culture after 24 hours.

Zeta potential determination

Apparent zeta potentials were measured using a Malvern Instruments Zetasizer Nano Z DLS instrument. 1 mL from 0.5 McFarland standardized microbial cultures in PBS (previously described) was added into a plastic disposable loading cell. This cell was washed thoroughly in deionized H_2O prior too, and between sample addition and changing. A voltage difference of 50 V was applied and the velocities of the cells were measured using M3-PALs (a patented laser interferometry technique involving phase analysis of scattered light). This allowed for calculation of electrophoretic mobility of the colloidal particles in solution (bacterial cells). From this, the zeta potentials and zeta potential distributions were determined. All zeta potential measurements were done at 25ºC.

Statistical analysis

Statistical analysis of all data groups was performed on commercially available software (R Open Source Statistical Programming). Statistical significance ($P < 0.05$) was determined between groups using a student's t-test.

Conclusions

This study revealed that clean stainless steel and gold substrates, which exhibited overall negative surface potentials, inhibited the attachment of both *P. aeruginosa* and MRSA even after 3 hours of static incubation under ambient conditions. Poly-L-lysine functionalization of surfaces led to positive surface potential shifts, with rapid microbial attachment observed after 30 minutes. Thus it can be concluded that negatively charged surfaces prevent *P. aeruginosa* and

MRSA microbial attachment for up to 3 hours. Significant shifts in cell surface potentials were observed for all microorganisms between stainless steel and gold substrates. This further confirms that substrate type plays an integral role in altering microbial cellular activity. Co-culturing led to significant changes in cell surface potential for MRSA cells on both stainless steel and gold surfaces. Thus, changes in MRSA cell surface potentials were more affected by co-culturing than by the substrate type. This is believed to be due to competitive effects as MRSAs growth is actively hindered by *P. aeruginosa* in co-culture. MRSAs metabolic activity is more affected by *P. aeruginosa*'s presence than by substrate type. This trend was not observed for *P. aeruginosa*. *P. aeruginosa* dominates over MRSA in co-culture and is believed to be metabolically less affected by its presence. This may explain why *P. aeruginosa*'s cell surface potential is more affected by substrate type and less by co-culturing.

CI and RIR calculations from selective plating experiments further revealed the inhibitory and competitive effects of *P. aeruginosa* on MRSAs activity and growth.

Zeta potential experiments represent the only realistic cell surface potential data as *P. aeruginosa* and MRSA are in their native state, as compared to being dead and dried on stainless steel and gold surfaces for FM-KPFM. Thus, the appearance of positive cell surface membranes is irrelevant to any conclusions on actual living cell surface potentials that truly exist in a wound setting or on stainless steel or gold surfaces that may be found in a nosocomial setting. Thus, for FM-KPFM data only general trends in cell surface potential shifts can be accurately commented upon with regard to changes in substrate type or co-culturing. Zeta potential data showed all mono- and co-cultures to have small negative zeta potentials ranging from -12.233 mV to -13.483 mV (no significant difference between cultures). This agrees with data from previous zeta potential studies of *P. aeruginosa* and MRSA cells.

AFM analysis of representative cells from mono- and co-cultures revealed no significant changes in cell morphology in co-cultures. It does not appear that inhibition of MRSA by *P. aeruginosa* leads to structural changes in MRSA cells.

As an alternative to antimicrobials and antibiotics, electrical stimulation is being increasingly explored for the eradication of wound biofilms.[44] Stimulation of wound repair by electrical stimulation is gaining momentum in wound care management and is based on the hypothesis that a decrease in trans-epithelial potential in non-lesional epidermis induces an endogenous current epithelial electric field in wound.[45] The investigations of our study on the influence of mono- and co-cultures of virulent bacteria on the cell surface potential and the effects of substrate surface potential on microbial attachment using Kelvin probe force microscopy has the potential to address issues important to the development of wound healing strategies using electrotherapy. Importantly, the use of non-chemical methods for combating microbial infections does not further lead to antimicrobial resistance, and thus it is of paramount importance that electrotherapy research be further explored.

Acknowledgements

The authors sincerely thank the Natural Sciences and Engineering Research Council of Canada, the Ontario Ministry of Research and Innovation, and the Canada Foundation for Innovation for funding this study.

References

1. B. M. Peters, M. A. Jabra-Rizk, G. A. O'May, J. W. Costerton and M. E. Shirtliff, *Clinical microbiology reviews*, 2012, **25**, 193-213.
2. B. S. Scales and G. B. Huffnagle, *The Journal of pathology*, 2013, **229**, 323-331.

3. I. Pastar, A. G. Nusbaum, J. Gil, S. B. Patel, J. Chen, J. Valdes, O. Stojadinovic, L. R. Plano, M. Tomic-Canic and S. C. Davis, *PloS one*, 2013, **8**, e56846.

4. L. Yang, Y. Liu, T. Markussen, N. Hoiby, T. Tolker-Nielsen and S. Molin, *FEMS immunology and medical microbiology*, 2011, **62**, 339-347.

5. J. Kim, H. D. Park and S. Chung, *Molecules (Basel, Switzerland)*, 2012, **17**, 9818-9834.

6. T. Julian, A. Singh, J. Rousseau and J. S. Weese, *BMC research notes*, 2012, **5**, 193.

7. C. Harrison-Balestra, A. L. Cazzaniga, S. C. Davis and P. M. Mertz, *Dermatologic surgery : official publication for American Society for Dermatologic Surgery [et al.]*, 2003, **29**, 631-635.

8. A. N. Athanasopoulos, M. Economopoulou, V. V. Orlova, A. Sobke, D. Schneider, H. Weber, H. G. Augustin, S. A. Eming, U. Schubert, T. Linn, P. P. Nawroth, M. Hussain, H. P. Hammes, M. Herrmann, K. T. Preissner and T. Chavakis, *Blood*, 2006, **107**, 2720-2727.

9. M. E. Mulcahy, J. A. Geoghegan, I. R. Monk, K. M. O'Keeffe, E. J. Walsh, T. J. Foster and R. M. McLoughlin, *PLoS pathogens*, 2012, **8**, e1003092.

10. J. Palmer, S. Flint and J. Brooks, *Journal of industrial microbiology & biotechnology*, 2007, **34**, 577-588.

11. L. Allen, D. H. Dockrell, T. Pattery, D. G. Lee, P. Cornelis, P. G. Hellewell and M. K. Whyte, *Journal of immunology (Baltimore, Md. : 1950)*, 2005, **174**, 3643-3649.

12. S. L. Percival, C. Emanuel, K. F. Cutting and D. W. Williams, *International wound journal*, 2012, **9**, 14-32.

13. D. P. Allison, N. P. Mortensen, C. J. Sullivan and M. J. Doktycz, *Wiley interdisciplinary reviews. Nanomedicine and nanobiotechnology*, 2010, **2**, 618-634.

14. S. Lu, G. Walters, R. Parg and J. R. Dutcher, *Soft matter*, 2014, **10**, 1806-1815.

15. J. Park, J. Yang, G. Lee, C. Y. Lee, S. Na, S. W. Lee, S. Haam, Y. M. Huh, D. S. Yoon, K. Eom and T. Kwon, *ACS nano*, 2011, **5**, 6981-6990.

16. S. Takeda, F. Ohkawa, H. Shu-Ping, T. Sakurai, S. Jin, H. Fuda, K. Sueoka and H. Chiba, *Sensors Journal, IEEE*, 2013, **13**, 3449-3453.

17. N. Kodera, D. Yamamoto, R. Ishikawa and T. Ando, *Nature*, 2010, **468**, 72-76.

18. W. Melitz, J. Shen, A. C. Kummel and S. Lee, *Surface Science Reports*, 2011, **66**, 1-27.

19. B. Moores, F. Hane, L. Eng and Z. Leonenko, *Ultramicroscopy*, 2010, **110**, 708-711.

20. A. L. Domanski, E. Sengupta, K. Bley, M. B. Untch, S. A. Weber, K. Landfester, C. K. Weiss, H. J. Butt and R. Berger, *Langmuir : the ACS journal of surfaces and colloids*, 2012, **28**, 13892-13899.

21. L. Collins, S. Jesse, J. I. Kilpatrick, I. V. Vlassiouk, A. Tselev, S. A. L. Weber, S. Jesse, S. V. Kalinin, and B. J. Rodriguez, *Applied physics letters*, 2014, **104**, 133103.

22. N. Kobayashi, H. Asakawa, and T. Fukuma, *Review of scientific instruments*, 2010, **81**, 123705.

23. L. Collins, S. Jesse, J. I. Kilpatrick, A. Tselev, O. Varenyk, M. B. Okatan, S. A. L. Weber, A. Kumar, N. Balke, S. V. Kalinin, and B. J. Rodriguez, *Nature communications*, 2014, **5**, doi: 10.1038/ncomms4871.

24. I. Lee, E. Chung, H. Kweon, S. Yiacoumi and C. Tsouris, *Colloids and surfaces. B, Biointerfaces*, 2012, **92**, 271-276.

25. E. Chung, S. Yiacoumi, I. Lee and C. Tsouris, *Environmental science & technology*, 2010, **44**, 6209-6214.

26. C. C. Tsai, H. H. Hung, C. P. Liu, Y. T. Chen and C. Y. Pan, *PloS one*, 2012, **7**, e33849.

27. G. S. Lorite, R. Janissen, J. H. Clerici, C. M. Rodrigues, J. P. Tomaz, B. Mizaikoff, C. Kranz, A. A. de Souza and M. A. Cotta, *PloS one*, 2013, **8**, e75247.

28. Y. J. Oh, W. Jo, Y. Yang and S. Park, *Applied Physics Letters*, 2007, **90**, -.

29. W. Zhang, J. Hughes and Y. Chen, *Applied and environmental microbiology*, 2012, **78**, 3905-3915.

30. B. Gottenbos, D. W. Grijpma, H. C. van der Mei, J. Feijen and H. J. Busscher, *The Journal of antimicrobial chemotherapy*, 2001, **48**, 7-13.

31. A. Pranzetti, S. Mieszkin, P. Iqbal, F. J. Rawson, M. E. Callow, J. A. Callow, P. Koelsch, J. A. Preece and P. M. Mendes, *Advanced materials (Deerfield Beach, Fla.)*, 2013, **25**, 2181-2185.

32. C. Martin-Granados and C. D. McCaig, *Advances in wound care*, 2014, **3**, 127-138.

33. C. Ayala-Torres, N. Hernández, A. Galeano, L. Novoa-Aponte and C.-Y. Soto, *Ann Microbiol*, 2013, 1-7.

34. P. Wang, T. B. Kinraide, D. Zhou, P. M. Kopittke and W. J. Peijnenburg, *Plant physiology*, 2011, **155**, 808-820.

35. M. Gross, S. E. Cramton, F. Gotz and A. Peschel, *Infection and immunity*, 2001, **69**, 3423-3426.

36. B. A. Jucker, H. Harms and A. J. Zehnder, *Journal of bacteriology*, 1996, **178**, 5472-5479.

37. A. P. Macho, A. Zumaquero, I. Ortiz-Martin and C. R. Beuzon, *Molecular plant pathology*, 2007, **8**, 437-450.

38. M. Tariq, C. Bruijs, J. Kok and B. P. Krom, *Applied and environmental microbiology*, 2012, **78**, 2282-2288.

39. R. L. Soon, R. L. Nation, S. Cockram, J. H. Moffatt, M. Harper, B. Adler, J. D. Boyce, I. Larson and J. Li, *The Journal of antimicrobial chemotherapy*, 2011, **66**, 126-133.

40. A. E. van Merode, H. C. van der Mei, H. J. Busscher and B. P. Krom, *Journal of bacteriology*, 2006, **188**, 2421-2426.

41. A. Roosjen, H. J. Busscher, W. Norde and H. C. van der Mei, *Microbiology (Reading, England)*, 2006, **152**, 2673-2682.

42. L. A. Rawlinson, J. P. O'Gara, D. S. Jones and D. J. Brayden, *Journal of medical microbiology*, 2011, **60**, 968-976.

43. E. Klodzinska, M. Szumski, K. Hrynkiewicz, E. Dziubakiewicz, M. Jackowski and B. Buszewski, *Electrophoresis*, 2009, **30**, 3086-3091.

44. C. Watters and M. Kay, in *Antibiofilm Agents*, eds. K. P. Rumbaugh and I. Ahmad, Springer Berlin Heidelberg, 2014, vol. 8, ch. 19, pp. 425-447.

45. V. J. Moulin, J. Dube, O. Rochette-Drouin, P. Levesque, R. Gauvin, C. J. Roberge, F. A. Auger, D. Goulet, M. Bourdages, M. Plante and L. Germain, *Advances in wound care*, 2012, **1**, 81-87.

Figure Captions

Fig. 1. Topography and surface potential maps of mono- and co-cultures on poly-L-lysine coated stainless steel and gold surfaces.

Fig. 2. Electrical surface potentials of surface substrates and cell membranes. Mono- and co-culture measurements were taken from poly-L-lysine treated surfaces after 30 minutes of incubation. Surface potentials were not homogenously and equally distributed across substrate surfaces. This charge heterogeneity was more apparent on clean (non-functionalized) surfaces and may explain the appearance of larger error bars compared to poly-L-lysine functionalized surfaces. MRSA = Methicillin Resistant Staphylococcus aureus, PA = P. aeruginosa, SS = Stainless steel, * = significant difference ($P < 0.05$). Note that SS and Gold substrates without the preface "Clean" are poly-L-lysine functionalized.

Fig. 3. Competitive index (CI) and relative increase ratios (RIR). CI was calculated as the ratio of bacterial burdens between the resistant strain (in this case *P. aeruginosa*, because of its known ability to affect MRSA) and susceptible strain (MRSA), divided by the corresponding CFU/mL ratio of the inoculums. Co-culture (after 24 hours) data from selective dilution plating experiments was used to calculate CI (CI = (CFU/mL MRSA at 24 hours/CFU/mL *P. aeruginosa* at 24 hours) / (ratio of CFU/mL of MRSA and PA inoculums). RIR was calculated using mono-culture information from selective dilution plating experiments after 24 hours, and is calculated in a similar fashion to CI.

Fig. 4. Zeta potential measurements of MRSA and P. aeruginosa (PA) mono-cultures and 1:1 co-culture. Measurements were taken at 25ºC with an applied voltage of 50 V. Zeta potential was determined using phase analysis of scattered light by the colloidal particles suspended in the PBS medium.

Tables and captions

Table 1 Average cell dimensions as determined by AFM measurements. A total of 15 representative cells from each cell type/culture type adhered to gelatin-coated mica (0.005 g/mL) were used for measurements. Significance between dimensions, lengths, and widths between cells are noted below.

Cell Type	Length	Width	Diameter	Significant Difference
MRSA	---	---	1.588 µm +/- 0.269 µm	No
MRSA (co-culture)			1.544 µm +/- 0.306 µm	No
P. aeruginosa	2.496 µm +/- 0.351 µm	1.127 µm +/- 0.101 µm	---	Length: No Width: No
P. aeruginosa (co-culture)	2.649 µm +/- 0.245 µm	1.147 µm +/- 0.231 µm	---	Length: No Width: No

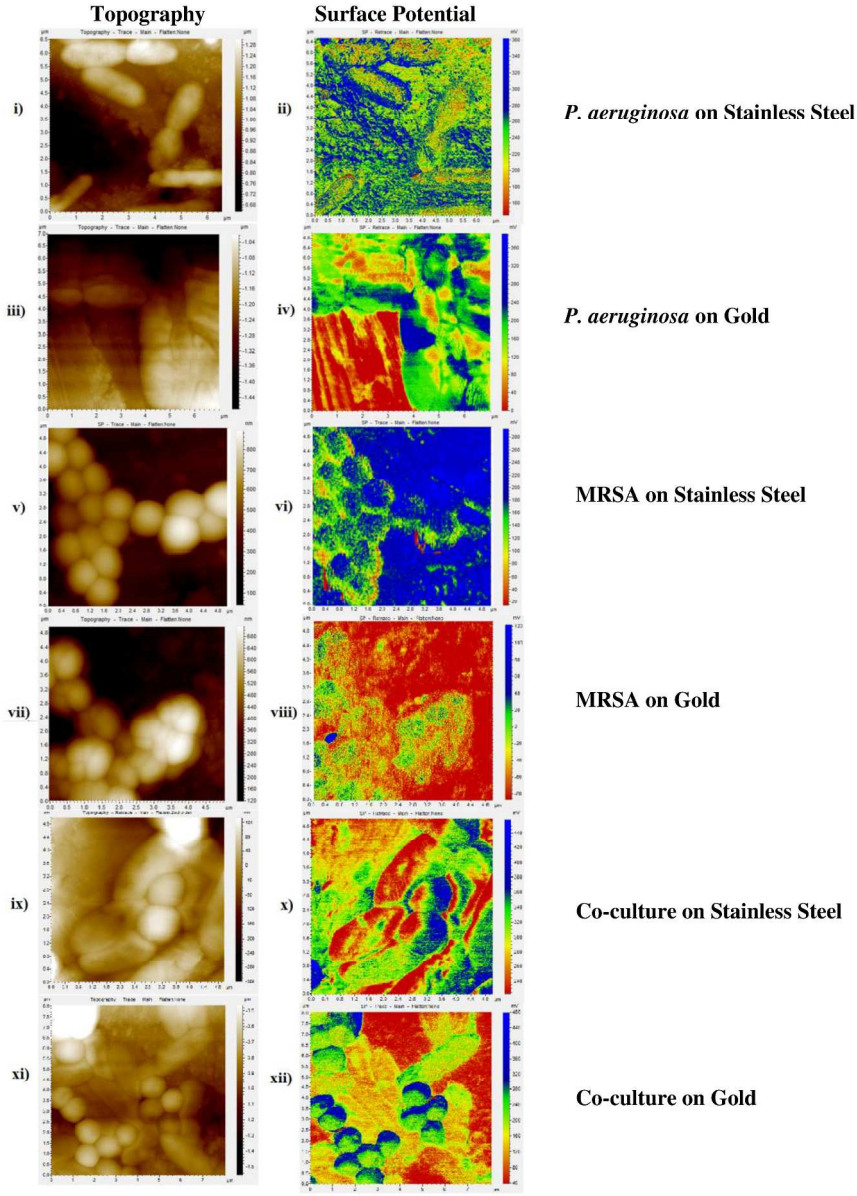

271x373mm (300 x 300 DPI)

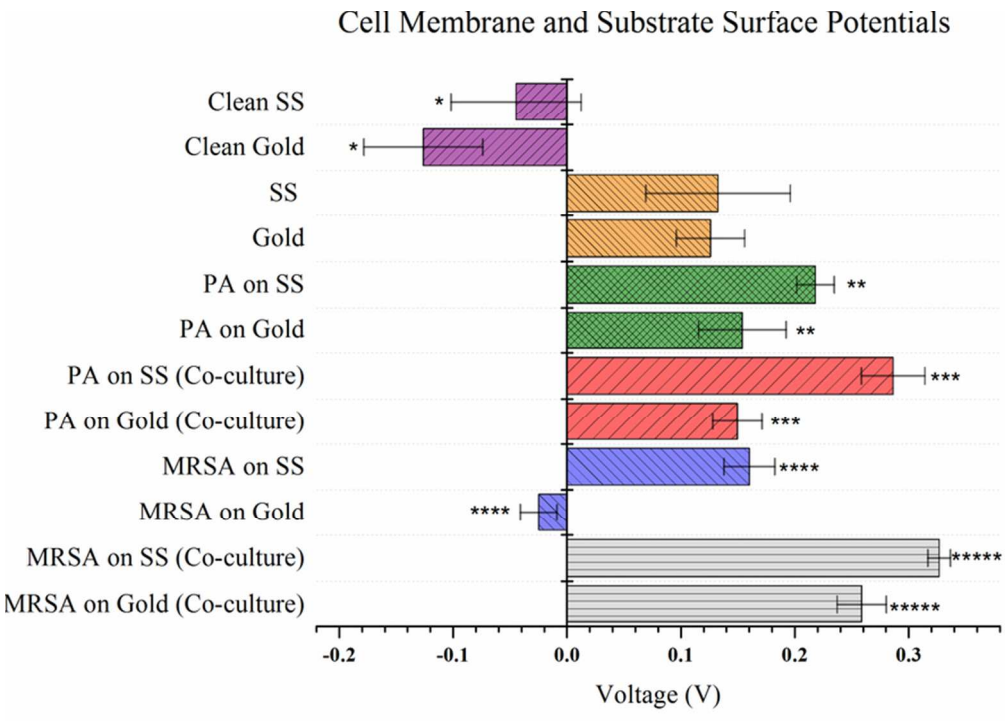

74x53mm (300 x 300 DPI)

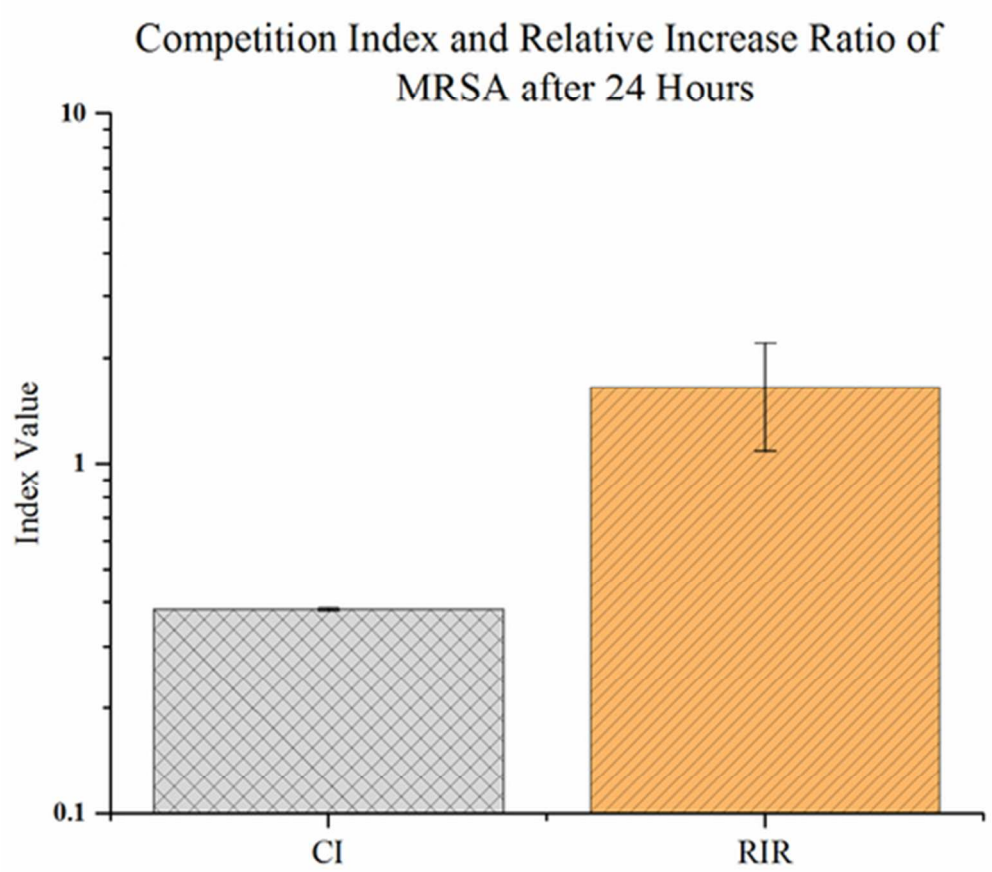

43x37mm (300 x 300 DPI)

Cell Type	Length	Width	Diameter	Significant Difference
MRSA	---	---	1.588 µm +/- 0.269 µm	No
MRSA (co-culture)			1.544 µm +/- 0.306 µm	No
P. aeruginosa	2.496 µm +/- 0.351 µm	1.127 µm +/- 0.101 µm	---	Length: No Width: No
P. aeruginosa (co-culture)	2.649 µm +/- 0.245 µm	1.147 µm +/- 0.231 µm	---	Length: No Width: No

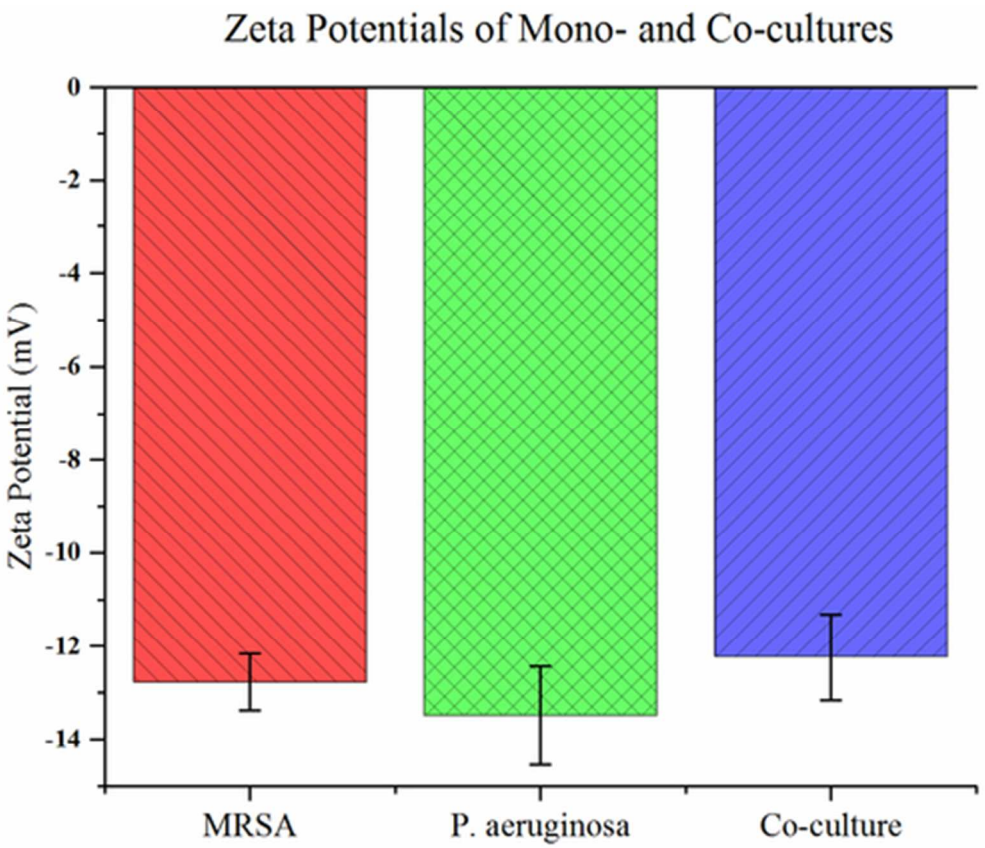

41x35mm (300 x 300 DPI)

Graphical Abstract

Quantitative nanoscale surface potential measurement of individual pathogenic bacterial cells for understanding the adhesion kinetics using Kelvin probe force microscopy

KPFM of Methicillin-Resistant *Staphylococcus aureus* on Poly-L-Lysine Coated Stainless Steel Surfaces

AFM Topography

KPFM Surface Potential